HHS Public Access

Author manuscript

*Nat Neurosci*. Author manuscript; available in PMC 2013 October 01.

Published in final edited form as:

*Nat Neurosci*. 2013 April ; 16(4): 456–463. doi:10.1038/nn.3353.

# CaMKII is a novel regulator of diacylglycerol lipase-α and striatal endocannabinoid signaling

**Brian C. Shonesy**[1], **Xiaohan Wang**[2,3], **Kristie L. Rose**[4], **Teniel S. Ramikie**[2,5], **Victoria S. Cavener**[2], **Tyler Rentz**[1], **Anthony J. Baucum II**[1], **Nidhi Jalan-Sakrikar**[1], **Ken Mackie**[7], **Danny G. Winder**[1,2,6], **Sachin Patel**[1,2,5,6,*], and **Roger J. Colbran**[1,2,6,*]

[1]Department of Molecular Physiology and Biophysics, Vanderbilt University School of Medicine, Nashville, TN, USA

[2]Vanderbilt Brain Institute, Vanderbilt University School of Medicine, Nashville, TN, USA

[3]Vanderbilt International Scholar Program, Vanderbilt University School of Medicine, Nashville, TN, USA

[4]Department of Biochemistry, Vanderbilt University School of Medicine, Nashville, TN, USA

[5]Department of Psychiatry, Vanderbilt University School of Medicine, Nashville, TN, USA

[6]Vanderbilt-Kennedy Center for Research on Human Development, Vanderbilt University School of Medicine, Nashville, TN, USA

[7]The Gill Center and the Department of Psychological & Brain Sciences, Indiana University, Bloomington, IN, USA

## Abstract

The endocannabinoid 2-arachidonoylglycerol (2-AG) mediates activity-dependent depression of excitatory neurotransmission at central synapses; however, the molecular regulation of 2-AG synthesis is not well understood. Here we identify a novel functional interaction between the 2-AG synthetic enzyme diacylglycerol lipase-α (DGLα) and calcium/calmodulin dependent protein kinase II (CaMKII). Activated CaMKII interacts with the C-terminal domain of DGLα, phosphorylates two serine residues, and inhibits DGLα activity. Moreover, CaMKII inhibition augments short-term retrograde eCB signaling at striatal glutamatergic synapses. Consistent with an inhibitory role for CaMKII in synaptic 2-AG synthesis, *in vivo* genetic inhibition of CaMKII



*Address correspondence to either: Roger J. Colbran; Rm. 702 Light Hall, Vanderbilt University School of Medicine, Nashville, TN 37232-0615 (Tel: 615-936-1630. Fax: 615-322-7236. roger.colbran@vanderbilt.edu) or Sachin Patel; 724B Robinson Research Building, Vanderbilt University School of Medicine, Nashville, TN 37232 (Tel.: 615-936-7768. Fax: 615-322-1462. sachin.patel@vanderbilt.edu).

Author Contributions

BCS and AJB performed all of the immunoprecipitation studies, and LC/MS quantification of striatal lipid levels. BCS performed all of the DGL activity assays. VSC carried out the GST-cosedimentation assay. BCS and XW generated the GST-fusion proteins and DGLα mutants and performed the phosphorylation site identification studies. BCS and KLR performed the LC/MS analysis of phosphorylation sites. BCS, TR and SP conducted the electrophysiology experiments. BCS and TSR carried out the behavioral experiments. BCS analyzed data from all experiments. NJS performed the T286 phosphorylation measurements in HEK293 cells. KM contributed the DGL antibodies. BCS, DGW, SP and RJC designed the experiments. BCS, SP, and RJC prepared the manuscript with input from all other authors.

increases striatal DGL activity and basal 2-AG levels. Moreover, blockade of 2-AG breakdown using concentrations of JZL-184 that have no significant effect in wild type mice produces a hypo-locomotor response in mice with reduced CaMKII activity. These findings provide novel mechanistic insight into the molecular regulation of striatal eCB signaling with implications for physiological control of motor function.

Motor function and action selection are controlled by the basal ganglia[1, 2]. Cortical inputs form glutamatergic synapses on "direct" and "indirect" pathway striatal medium spiny neurons (MSNs) provide the major excitatory drive to the basal ganglia to facilitate and inhibit motor activity, respectively[3]. Endocannabinoid (eCB) signaling plays a prominent role in the modulation of synaptic efficacy at corticostriatal synapses[4-7]. In contrast to conventional neurotransmitter release from stores in presynaptic vesicles, eCBs are synthesized and released on-demand from postsynaptic neurons in an activity-dependent manner. These retrograde transmitters diffuse to presynaptic boutons and activate cannabinoid CB1 receptors (CB1Rs) to suppress glutamate release in many brain regions, including the striatum[4, 8]. Moreover, abnormal striatal eCB signaling has been linked to several movement disorders, including Parkinson's disease[9], Tourette's syndrome[10], and Huntington's disease[11].

The two best-studied eCBs are anandamide[12] and 2-arachidonylglycerol (2-AG)[13]. 2-AG can be synthesized by two *sn*-1 specific diacylglycerol lipase isoforms, DGLα or DGLβ, and is significantly more abundant in the striatum[14]. While DGLβ has important roles during development[15], DGLα plays a dominant synaptic role in the mature brain[7, 16, 17]. DGLα appears to be regulated by calcium and co-factors such as glutathione[18], and recent studies suggest that interactions with Homer proteins are critical for subcellular targeting of DGLα[19].

Three different mechanisms can initiate activity-dependent synaptic depression by 2-AG[7, 20, 21, 22]. First, postsynaptic depolarization can induce pure calcium and DGLα-dependent 2-AG synthesis and release[23, 24]. This process is termed **d**epolarization-induced **s**uppression of either **e**xcitation[25] (DSE, i.e., depression of glutamatergic transmission) or **i**nhibition[23] (DSI, i.e., depression of GABAergic transmission). Second, pairing activation of $G_{q/11}$-protein-coupled receptors, including group I metabotropic glutamate receptors (mGluRs), with less robust calcium signals triggers 2-AG mobilization in a process termed 'calcium-assisted receptor driven 2-AG release'[26-28]. Finally, robust mGluR activation alone can initiate 2-AG signaling in a calcium-independent manner[29]. However, molecular mechanisms regulating DGLα activity in these different situations are not well understood.

Here, we define a novel mechanism for DGLα regulation by calcium/calmodulin-dependent protein kinase II (CaMKII). CaMKII plays critical roles in synaptic plasticity by regulating a broad range of proteins by phosphorylation and/or activity-dependent targeting. We now show that CaMKIIα binds to and phosphorylates DGLα, and inhibits 2-AG synthesis *in vitro*. Biochemical and electrophysiological data are consistent with a model in which CaMKIIα limits calcium-dependent eCB signaling at glutamatergic synapses onto both direct and indirect pathway MSNs. Moreover, behavioral studies indicate that CaMKIIα is a

negative regulator of eCB signaling *in vivo*. Our data provide novel insights into fundamental mechanisms regulating eCB signaling at central synapses.

## Results

### CaMKII interacts with DGL α

We initially screened for modulators of striatal DGLα by characterizing the DGLα interactome in mouse striatum using a shotgun proteomics approach. DGLα was immunoprecipitated from solubilized adult mouse striatal extracts. Immune complexes were resolved using SDS-PAGE and proteins in excised gel lanes were digested with trypsin. Extracted peptides were analyzed by LC-coupled tandem mass spectrometry (LC-MS/MS) and matched to the UniProt database (see Methods). Multiple CaMKIIα and CaMKIIβ peptides were detected along with peptides derived from several other proteins (Supplementary Table 1). We confirmed that CaMKIIα interacts with DGLα by immunoblotting striatal DGLα immune complexes with an anti-CaMKIIα antibody (Fig 1a). Importantly, no CaMKIIα was detected in control IgG complexes (Fig 1a), demonstrating the interaction specificity. In order to confirm the interaction and test the isoform specificity of CaMKII-DGL binding, we expressed CaMKIIα or CaMKIIβ with either DGLα or DGLβ proteins containing a C-terminal V5-epitope tag in HEK293T cells. We found that DGLα-V5, but not DGLβ-V5, immune complexes contained CaMKIIα (Fig 1b). Moreover, both CaMKIIα and CaMKIIβ could specifically associate with recombinant DGLα-V5 (Fig. 1c).

While amino acid sequences of DGLα and DGLβ are very similar through the transmembrane and catalytic domains, DGLα contains a unique C-terminal domain extension (Fig. 1d). Since CaMKII interacts with DGLα but not DGLβ, and the formation of physiological CaMKII complexes is often enhanced by $Thr^{286}$ autophosphorylation of CaMKIIα[30, 31], which also generates constitutive CaMKIIα activity[32], we tested the hypothesis that $Thr^{286}$ autophosphorylated CaMKIIα directly interacts with the unique C-terminal domain of DGLα (residues 761–1042). Indeed, purified $Thr^{286}$ autophosphorylated CaMKIIα specifically bound to a purified glutathione S-transferase (GST) fusion protein containing the DGLα C-terminal domain (Fig. 1d). To further explore the role of $Thr^{286}$ autophosphorylation in modulating CaMKIIα interactions with full-length DGLα, we co-expressed full-length DGLα-V5 with either WT CaMKIIα or a Thr286 to Ala (T286A) mutant of CaMKIIα that cannot undergo $Thr^{286}$ autophosphorylation. WT CaMKIIα becomes partially phosphorylated at $Thr^{286}$ following expression in heterologous cells (Supplementary Fig. 2), and the T286A mutation significantly reduced CaMKII association with DGLα-V5 (Fig. 1e). Taken together, these data indicate that CaMKIIα is a novel DGLα associated protein, and that the interaction is enhanced by CaMKIIα $Thr^{286}$ autophosphorylation.

### CaMKIIα phosphorylates DGLα at $Ser^{808}$ and $Ser^{782}$

Since CaMKII phosphorylates many binding partners[33, 34], we compared the phosphorylation of DGL isoforms by CaMKIIα. DGLα-V5 or DGLβ-V5 were immuno-purified from transfected HEK293T cell lysates using a V5 antibody and then incubated with [$\gamma$-$^{32}$P]ATP, either alone or following addition of purified, activated CaMKIIα.

Autoradiography of SDS-polyacrylamide gels analyzing reactions containing both DGLα-V5 and CaMKIIα revealed a ≈116 kDa $^{32}$P-labeled protein that aligns with the DGLα-V5 band on the anti-V5 western blot, as well as a ≈55 kDa band corresponding to autophosphorylated CaMKIIα (Fig. 2a). The 116 kDa $^{32}$P-labeled protein was not detected in control reactions lacking either DGLα or CaMKIIα. Furthermore, there was no detectable $^{32}$P incorporation into DGLβ-V5 in the presence or absence of CaMKIIα, consistent with our finding that DGLβ does not interact with CaMKII. Thus, CaMKIIα selectively phosphorylates DGLα, but not DGLβ.

In order to identify CaMKII phosphorylation sites, full length DGLα-V5 was immunoprecipitated from transfected cell lysates and incubated in the presence of ATP with or without activated CaMKIIα. LC-MS/MS analysis of proteolytic digests of the DGLα-V5 detected a total of 10 phosphorylated serine/threonine residues in one or both samples (Table 1). All but one of these sites were located within the unique C-terminal domain of DGLα (Fig. 2c). Sites detected in the absence of added CaMKII may be phosphorylated by endogenous HEK293 cell kinases either in intact cells or *in vitro*. Notably, only Ser$^{782}$ and Ser$^{808}$ showed a substantial increase in phosphorylation following the incubation with CaMKIIα (Table 1, Fig 2b).

In order to confirm that CaMKII phosphorylates DGLα, a series of GST fusion proteins containing C-terminal domain fragments of DGLα (Fig. 2c), or GST alone as a control, were incubated with [γ-$^{32}$P]ATP in the presence of purified activated CaMKIIα. Two fragments, containing residues 761–1042 and 761–870, were phosphorylated with similar stoichiometries (Fig. 2d), yet a fragment containing residues 871–1042 and two other fragments were not significantly phosphorylated. These data indicate that the CaMKII phosphorylation site(s) reside between residues 761 and 870, consistent with the LC-MS/MS data identifying Ser$^{782}$ and Ser$^{808}$ as CaMKII phosphorylation sites in the full-length protein. To determine whether these sites were selectively phosphorylated *in vitro*, Ser$^{808}$ and Ser$^{782}$ were mutated to alanine individually and in combination. The single mutation of Ser$^{808}$ to alanine substantially reduced the extent of phosphorylation by CaMKII, whereas the Ser$^{782}$ to alanine mutation had a more modest effect. Double mutation of Ser$^{782}$ and Ser$^{808}$ to alanines reduced CaMKII phosphorylation to levels that were not significantly different from the GST control. In combination, these data indicated that Ser$^{808}$ is phosphorylated to a higher stoichiometry than Ser$^{782}$ (Fig 2e,f; See Supplemental Figure 1b for whole gel). To determine whether CaMKII phosphorylates these sites in intact cells, we purified DGLα-V5 from lysates of HEK293T cells with or without co-expression of constitutively active CaMKIIα and analyzed tryptic digests using a targeted LC-MS/MS approach. Phosphorylation of Ser$^{808}$ and Ser$^{782}$ was detected in digests of DGLα co-expressed with CaMKIIα, but not in digests of DGLα expressed alone (Supplementary Figure 3). Notably, Ser$^{808}$ and Ser$^{782}$ are conserved across a broad range of vertebrate species (Fig. 2g). In combination, these data show that CaMKIIα selectively phosphorylates Ser$^{808}$ and Ser$^{782}$ in the unique C-terminal domain of DGLα.

## CaMKII inhibits DGL activity *in vitro*

To begin to explore the functional consequences of DGLα phosphorylation at $Ser^{782}$ and $Ser^{808}$, we assayed the activities of full length WT or S782E/S808E DGLα proteins in membrane fractions from transfected HEK293T cells using various concentrations of the physiological DGL substrate, 1-steroyl-2-arachidonoylglycerol (SAG) (see Methods). Mutations of phosphorylation sites to glutamate often mimic the phosphorylated form. This phosphomimetic mutation significantly decreased the apparent $V_{max}$ of 2-AG production without affecting the apparent $K_m$ (Fig 3a). After subtracting background activity in membranes from mock-transfected cells, the S782E/S808E double mutation reduced the $V_{max}$ by ≈40%. These data suggest that CaMKIIα could inhibit DGLα activity through phosphorylation at $Ser^{782}$ and $Ser^{808}$.

We next investigated the regulation of striatal DGL. Production of 2-AG from a striatal membrane fraction was approximately linear with time, SAG concentration-dependent, and blocked by the DGL inhibitor tetrahydrolipstatin (THL 1 μM; Supplemental figure 4). This activity was inhibited by addition of recombinant activated CaMKIIα in the presence of ATP (10 min, 30°C) in a concentration-dependent manner which was statistically significant with ≥500 nM CaMKIIα (Fig 3b). Heat-inactivation of the CaMKII (70°C, 30 min) prevented the inhibition of DGL activity (Fig 3c).

We further explored the role of CaMKII in regulating striatal DGL activity. Since $Thr^{286}$ autophosphorylation activates CaMKIIα and facilitates CaMKII-DGLα binding, we tested the effect of a homozygous $Thr^{286}$ to Ala knockin mutation (which reduces CaMKII activity due to the lack of $Thr^{286}$ autophosphorylation[35, 36]) on striatal DGLα activity. DGL activity in striatal membranes from $CaMKII\alpha^{T286A/T286A}$ mice (hereinafter referred to as T286A-KI mice) was significantly *higher* than the activity in membrane fractions from WT littermates (Fig 3d), consistent with the hypothesis that WT CaMKII was inhibiting DGLα. We next investigated whether the reduced CaMKII activity and enhanced DGLα activity in T286A-KI mice affected total endogenous levels of striatal 2-AG. Notably, levels of 2-AG in dorsolateral striatal tissue from T286A-KI mice were significantly *increased* relative to their WT littermates (Fig 3e). These increased levels of 2-AG do not appear to reflect an impairment of 2-AG breakdown into arachidonic acid and glycerol by the presynaptic monoacylglycerol lipase (MGL)[37] because there was no difference in arachidonic acid levels in WT and T286A-KI tissue (Fig 3e). However, further studies are needed to conclusively exclude CaMKIIα effects on MGL. Moreover, there was no difference in total striatal levels of anandamide between genotypes (Fig 3g). Taken together, these data show that CaMKIIα inhibits DGLα *in vitro*, and that mice with impaired CaMKIIα activity have increased DGL activity and a selective increase in striatal 2-AG levels *in vivo*. Thus, CaMKIIα is a negative-regulator of 2-AG signaling in the striatum.

## CaMKII negatively modulates striatal DSE

Since our data indicate that CaMKIIα constrains DGLα activity in vivo, we tested the hypothesis that CaMKII modulates 2-AG-mediated synaptic signaling in the striatum. We focused on DSE, a purely $Ca^{2+}$-dependent read-out of retrograde 2-AG signaling[38]. Depolarization of 8 out of 8 randomly selected MSNs in the dorsolateral striatum resulted in

a short-term depression of evoked excitatory postsynaptic currents (eEPSCs), and this depression was blocked by the CB1R antagonist rimonabant (Supplemental Fig 5a-c). Since emerging evidence suggests that striatal endocannabinoid-dependent long-term depression may be specific to indirect pathway (D2 receptor expressing) MSNs[21, 39, 40], we examined DSE in slices from D2-eGFP BAC transgenic mice, which express eGFP in indirect pathway MSNs[41]. Significant DSE was induced in both D2(+) and D2(−) MSNs by as little as a 3 s depolarization, although longer depolarizations induced more robust DSE in both cell types (Supplemental Fig 5d-g). Comparison of DSE in D2(−) and D2(+) MSNs across all depolarization times by 2-way ANOVA failed to detect a significant cell-type by depolarization time interaction, indicating that the magnitude of DSE is similar in both cell types.

We investigated the role of CaMKII in striatal DSE, by comparing DSE in WT and T286A-KI mice with redcued CaMKII activity (see above) that both also carry the D2-eGFP BAC transgene. DSE was enhanced in D2(−) MSNs in T286A-KI mice relative to their WT littermates (Fig 4a-b), consistent with the increased DGL activity and striatal 2-AG levels in these mice. We also investigated the role of CaMKII in DSE by perfusing an inhibitory peptide (AIP, 10 μM) in to the postsynaptic cell via the recording pipette that inhibits both $Ca^{2+}$-dependent and –independent CaMKII activity. Similar to the effect of T286A-KI mutation, AIP caused a significant enhancement of DSE in WT D2(−) MSNs (Fig 4a,b). Although the T286A-KI mutation had no effect on DSE in D2(+) MSNs, intracellular perfusion of AIP also significantly enhanced DSE in D2(+) MSNs (Fig 4c,d). Taken together, these data suggest cell-specific differences between direct and indirect pathway MSNs in either how CaMKII is regulated or how it interacts with the 2-AG signaling pathway. Furthermore, the fact that AIP was applied only to the postsynaptic cell indicates that DSE is modulated by postsynaptic CaMKII. Consistent with this interpretation, there is no change in presynaptic CB1 receptor signaling in T286A-KI mice, as evidence by a similar decrease of eEPSCs in MSNs from WT and T286A-KI mice following bath application of WIN55,212-2 (3 μM), a CB1R agonist (Supplementary Fig 6g).

Synthesis and release of 2-AG can also be induced by activation of group I mGluRs in combination with a depolarization-induced $Ca^{2+}$ signal[26-28]. Although still requiring DGLα, this mode of 2-AG release also involves signaling via phospholipase C-β (PLCβ)[27, 28], and in some cases may be $Ca^{2+}$ independent[42]. To determine if CaMKII plays a role in these pathways, slices from WT and T286A-KI mice were pretreated with the mGluR1/5 agonist DHPG (10 μM) prior to DSE induction. Notably, there was no significant difference in DSE induced by either a 10 s (Fig 4e-h) or 3 s (Supplemental Fig 6a-d) depolarization between T286A-KI mice and their WT littermates in either D2(−) or D2(+) MSNs in the presence of DHPG. Thus, the lack of DSE enhancement in T286A-KI mice in the presence of DHPG was not because DSE was maximally induced by a 10 sec depolarization. In addition, we saw no effect of postsynaptic AIP loading in D2(−) cells using a 3 sec depolarization in DHPG-treated slices (Supplemental Fig 6e,f). Together these results suggest that the mGluR1/5 activation overcomes the negative modulatory role of postsynaptic CaMKII in striatal 2-AG release.

### T286A-KI mice have enhanced sensitivity to MGL inhibition

Excitatory inputs to striatal MSNs play a critical role in controlling motor activity[43]. Moreover, previous work has demonstrated potent inhibitory effects of cannabinoids on movement[44]. After 2-AG is released, it is degraded by presynaptic MGL[37]; pharmacological inhibition of MGL with JZL-184 enhances 2-AG levels in the brain to reduce motor activity in a dose-dependent manner[45]. Therefore, in order to investigate the behavioral relevance of CaMKII modulation of 2-AG signaling *in vivo*, we compared the effects of JZL-184 in WT and T286A-KI mice. We reasoned that elevated striatal DGL activity in T286A-KI mice should amplify the build-up of 2-AG at synapses in T286A-KI mice in the presence of JZL-184. Thus, we predicted that JZL-184 should cause a more robust suppression of locomotor activity compared to WT littermates. To test this hypothesis, mice were habituated to a home cage monitoring-environment for 2 days, treated with vehicle and then monitored for 24-hr (see methods). Mice then received a submaximal dose of JZL-184 (12 mg/kg) and monitoring was continued for a further 24 hours. The distances traveled by these mice in each 1-hr period across the entire 48-hr period is shown in Fig. 5a. Although elevated baseline motor activity of vehicle-treated T286A-KI mice relative to WT littermates (due to an as yet unidentified mechanism) somewhat confounds direct comparisons, this submaximal dose of JZL-184 treatment significantly depressed motor activity in T286A-KI mice but not WT littermates (Fig 5b). On average, JZL-184 produced a 32±7% decrease in locomotor activity of T286A-KI mice, but had no net effect on the locomotor activity of WT mice (0.04±14.4%) (Fig 5c). This effect of JZL-184 in T286A-KI mice was not due to differences in habituation to the testing environment between genotypes because circadian locomotor patterns of T286A-KI and WT mice were reliable and stable when monitored for 3 consecutive days without any manipulations (Supplementary Fig 7). Importantly, there was no significant difference in eating, drinking, grooming, or sleeping in the home cage environment between genotypes, and JZL-184 treatment had no effect on these behaviors in either genotype (Fig 5d-g).

## Discussion

Here we identify a novel regulatory role for CaMKIIα in striatal eCB signaling. We found that CaMKIIα interacts with DGLα in mouse striatum, phosphorylates DGLα at $Ser^{782}$ and $Ser^{808}$, and inhibits DGLα activity. Furthermore, consistent with the expression pattern of DGL[20], DSE can be induced in both direct and indirect pathway MSNs, unlike striatal anandamide-mediated long-term depression[21, 39, 40],. Importantly, CaMKII inhibition enhances DSE in both cell types. These synaptic studies are consistent with our observation that CaMKIIα inhibits striatal DGLα activity *ex vivo*. Finally, we found that mice with a T286A-KI mutation are more sensitive to the locomotor suppressant effect of MGL inhibition, which may reflect an enhanced 2-AG synthetic pathway in these mice. Taken together these data suggest that CaMKIIα has important roles in controlling striatal functions by modulating $Ca^{2+}$-dependent 2-AG signaling at corticostriatal glutamatergic synapses.

Although Homer1 interacts with DGLα[19], interactions of DGLα with other proteins that may modulate the subcellular targeting or enzyme activity are poorly understood. Our initial

proteomics screen of striatal DGLα complexes detected Homer1 and several other postsynaptic density (PSD)-associated proteins including Shank3, a known binding partner of Homer1, PSD-95, PSD-93, SAPAP3 and SAPAP2. Further studies will be required to determine the biochemical basis and roles for these interactions with DGLα, but we speculate that they may contribute to the known targeting of DGLα to dendritic spines[20]. Notably, CaMKII was the only kinase detected in striatal DGLα immune complexes.

Residues 1–673 of DGLα are well conserved in DGLβ, but DGLα contains a unique C-terminal tail. We found that CaMKIIα can directly interact with the C-terminal tail of DGLα, and also interacts with full length DGLα, but not full length DGLβ. Using a proteomics-based approach, we also found that DGLα was phosphorylated at some level in HEK293 cells at several serine and threonine residues, mostly in the unique C-terminal tail, suggesting that DGL isoforms may be differentially regulated. These sites may be targeted by many kinases, but we found that CaMKIIα specifically phosphorylates $Ser^{782}$ and $Ser^{808}$ of DGLα. Moreover, mutation of $Ser^{782}$ and $Ser^{808}$ to glutamate, which mimics phosphorylation, decreases DGL activity *in vitro*. In agreement with this, we also show that incubation of striatal membranes with activated CaMKIIα reduces DGL activity by ~50% *in vitro*. Although further studies are required to fully understand the relative roles of CaMKII binding to DGLα and phosphorylation at $Ser^{782}$ and $Ser^{808}$, these data are the first to implicate CaMKIIα as a negative regulator of eCB synthesis via modulation of DGLα activity.

Previous studies indicate that endocannabinoids play distinct roles in long-term modulation of excitatory inputs onto direct and indirect pathway MSNs[21, 39]. In contrast, we found that striatal DSE can be expressed in both subpopulations of MSNs. Consistent with our biochemical data showing that CaMKIIα inhibits DGLα activity, DSE in both MSN subtypes was enhanced by acute postsynaptic blockade of CaMKII activity. These data show that postsynaptic CaMKII can inhibit eCB retrograde signaling at glutamatergic striatal synapses. Given the calcium dependence of both DGLα and CaMKII, our data suggest a scenario whereby strong calcium signals initiate eCB mobilization via activation of DGLα, but also recruit CaMKII to inhibit DGLα to limit and/or terminate eCB-mediated synaptic signaling.

Interestingly, the relative prominence of CaMKII feedback control of DGLα may vary subtly between striatal MSN subtypes. While postsynaptic perfusion of AIP to acutely inhibit both calcium-dependent and calcium-independent activity of both CaMKIIα and CaMKIIβ enhances DSE in both MSN subtypes, the inhibition of only calcium-independent CaMKIIα activity in T286A-KI mice selectively enhanced DSE in direct pathway MSNs. The T286A mutation of CaMKIIα does not affect calcium/calmodulin-stimulated CaMKIIα activity and does not directly affect CaMKIIβ. These apparently discrepant findings may have several explanations. First, this may reflect a difference between acute kinase inhibition compared to long-term genetic disruption in T286A-KI mice. Compensatory mechanisms may overcome the loss of calcium-independent CaMKIIα activity in indirect pathway T286A-KI MSNs, but not in direct pathway T286A-KI MSNs. Second, the “set point” of 2-AG signaling may differ in the two cell types, perhaps due to differences in the levels of $Thr^{286}$ autophosphorylation of CaMKIIα. Therefore, more robust inhibition of

CaMKII activity by AIP might be required to suppress DSE in MSNs with lower levels of $Thr^{286}$ autophosphorylation.

Neither acute CaMKII blockade nor the T286A-KI mutation affected calcium-assisted mGluR-mediated 2-AG release. The differential regulation of these distinct forms of eCB-mobilization by CaMKII may be related to the mechanistic differences in these two signaling pathways. DSE is mediated by calcium-dependent activation of DGLα, whereas calcium-assisted mGluR-mediated 2-AG signaling is mediated via calcium enhancement of PLCβ activity, which provides diacylglycerol substrate for DGLα. Moreover, these two forms of 2-AG mobilization may depend on distinct pools of DGLα[46]. For example, a complex between DGLα and mGluRs mediated by Homer proteins may recruit a specific pool of DGLα for mGluR-mediated 2-AG signaling[19]. Purely calcium-driven DSE may involve distinct pools of DGLα[46] that are not associated with mGluRs or Homer, but which can be regulated by CaMKII[47], perhaps associated with calcium channels, for example[47]. Thus, in this putative model, CaMKIIα may not be able to inhibit DGLα molecules in complex with mGluRs and Homer. Future studies will be required to determine the molecular basis for the differential regulation of calcium-dependent, and calcium-assisted mGluR driven, eCB mobilization by CaMKIIα. Although our biochemical and electrophysiological findings strongly support the conclusion that CaMKII regulates DGLα-mediated 2-AG synthesis, at this time we cannot rule out an additional role for CaMKII in 2-AG release.

Lastly, we have begun to evaluate the significance of CaMKIIα-eCB signaling interactions *in vivo* using T286A-KI mice. Inhibition of 2-AG hydrolysis using JZL-184 reduced locomotor hyperactivity in T286A-KI mice using a homecage monitoring system which reduces potential confounds of novelty/anxiety to the measurement of locomotor activity. Since T286A-KI mice have elevated DGL activity, one explanation for these data is that blockade of 2-AG hydrolysis results in enhanced 2-AG- and CB1-mediated inhibition of glutamatergic drive to direct pathway neurons in T286A-KI mice. Although enhanced suppression of direct pathway circuits in T286A-KI mice could explain the locomotor suppression, several caveats to this interpretation remain. Importantly, T286A mice exhibit a baseline hyperactive phenotype, which is unlikely to be explained by alterations in basal 2-AG signaling because the enhanced 2-AG levels and enhanced direct pathway DSE would predict a *hypo*-rather than *hyper*active phenotype. Furthermore, we cannot conclusively exclude contributions from deficits in spatial and working memory displayed by T286A-KI mice[35, 48] to the changes in locomotor activity. Nevertheless, these data clearly support the overall notion that CaMKIIα-eCB interactions occur *in vivo*, and could regulate striatal function under physiological and possibly pathophysiological conditions in which striatal CaMKIIα function is enhanced, such as experimental parkinsonism[49, 50].

In summary, these studies provide evidence for a novel functional link between CaMKIIα and 2-AG signaling in the striatum. The data indicate that CaMKIIα is a negative modulator of short-term calcium-dependent eCB signaling at corticostriatal glutamatergic synapses, adding to the diverse synaptic functions of CaMKII. Future studies need to be directed at understanding how distinct modes of 2-AG signaling are differentially regulated by CaMKII signaling and the precise molecular determinants of CaMKII modulation of DGLα activity.

Further exploration of these questions could provide novel strategies to fine-tune synaptic transmission in the central nervous system in multiple neurological and psychiatric disorders.

## Methods

### Animals

Male WT and homozygous CaMKIIα$^{T286A/T286A}$ mice[1] were generated by breeding heterozygous mice. CaMKIIα$^{T286A/WT}$ heterozygotes were crossed with drd2-eGFP BAC transgenic mice (hemizygous) to generate drd2-eGFP hemizygotes (drd2-eGFP$^{+}$) on a heterozygous CaMKIIα$^{T286A/WT}$ background. The drd2-eGFP$^{+}$/CaMKIIα$^{T286A/WT}$ mice were then bred with drd2-eGFP$^{-}$/CaMKIIα$^{T286A/WT}$ mice to produce the drd2-eGFP$^{+}$/CaMKIIα$^{WT/WT}$ and drd2-eGFP$^{+}$/CaMKIIα$^{T286A/T286A}$ used for electrophysiology experiments. All mice were on a C57Bl6 background and were housed on a 12 hr light-dark cycle with food and water ad libitum. Homozygous CaMKIIα$^{T286A/T286A}$ mice are referred to as T286A-KI mice throughout this paper. Behavioral experiments were performed at postnatal day 43–50, while biochemical and electrophysiological experiments were performed at postnatal days 21–27. All experiments with mice were approved by the Vanderbilt University Institutional Animal Care and Use Committee and were carried out in accordance with the NIH Guide for the Care and Use of Laboratory Animals.

### Cloning and Protein Expression

DGLα-V5 and DGLβ-V5 plasmids were generous gifts from Dr. Benjamin Cravatt (The Scripps Research Institute, La Jolla, CA). DGLα mutants were generated by site-directed mutagenesis, and verified by sequencing. GST-fusion proteins were generated by PCR amplification followed by restriction digest cloning into pGEX6P-1 using BamHI and XhoI sites. Vectors were transformed into BL21-DE3 pLysS E. coli, and purification was carried out as previously described[2]. Recombinant mouse CaMKIIα purified from baculovirus-infected Sf9 insect cells was autophosphorylated at Thr$^{286}$ essentially as described previously[2].

### Immunoprecipitation

**HEK293T cells—**Lysates were prepared in cold lysis buffer (2 mM Tris-HCl pH 7.5, 2 mM EDTA, 2 mM EGTA, 1% (v/v) Triton X-100, 1 mM DTT, 0.2 mM PMSF, 1 mM benzamidine, 10 μg/ml leupeptin, 10 μM pepstatin, 1 μM microcystin). Goat anti-V5 (Bethyl Laboratories, A190-119A, 1:5) was crosslinked to protein-G magnetic beads using dimethyl pimelimidate (DMP; 10.4 mg/ml) following manufacturers instructions (Dynabeads, Invitrogen). The beads were incubated with lysates overnight and were then washed with IP buffer (150 mM NaCl, 50 mM Tris-HCl pH 7.5 and 1% Triton X-100). Inputs and precipitates were resolved by SDS-PAGE and analyzed by western blotting using a rabbit anti-V5 (Bethyl Laboratories, A190-120A, 1:10,000), mouse anti-CaMKIIα 6G9 (Pierce, MA1-048, 1:3,000) or mouse anti-CaMKIIβ (Invitrogen, 13-9800, 1:3000).

**Mouse Striatum—**Mice were decapitated without anesthesia, and the striatum was homogenzied in lysis buffer (150 mM KCl, 50 mM Tris-HCl, 1% Triton X-100 (v/v), 1 mM

DTT, 0.2 mM PMSF, 1 mM benzamidine, 10 μg/ml leupeptin, 10 μM pepstatin, 1 mM $NaVO_4$, 1 mM NaF, and 1 μM microcystin). After centrifugation (9,000 × g,10 min), supernatants were incubated overnight with anti-DGLα (validated in previous studies[5, 6]), crosslinked to magnetic protein-G beads (see above). After washing with IP wash buffer, immune complexes were resolved by SDS-PAGE and either analyzed by western blotting or used for proteomic studies.

## GST Cosedimentation Assay

GST cosedimentation assays were performed as previously described[2].

## Proteomics Methods

For phosphorylation site analysis, DGLα was isolated from transfected HEK293 cells, phosphorylated by CaMKII (see below) and resolved by SDS-PAGE. Excised gel bands were incubated with 100 mM ammonium bicarbonate, pH 8, reduced with 4 mM DTT or TCEP, alkylated with 8 mM iodoacetamide and finally digested overnight with trypsin, elastase, or endoproteinase AspN (10 ng/μl; 37°C). Extracted peptides were reconstituted in 0.1% formic acid.

Peptide mixtures were fractionated on a C18 reverse phase column (360 μm O.D. × 100 μm I.D. Jupiter, 3 μm beads, 300 Å, Phenomenex) equipped with a laser-pulled emitter tip (flow rate: 500 nl/min). Mobile phase solvents consisted of 0.1% formic acid, 99.9% water (solvent A) and 0.1% formic acid, 99.9% acetonitrile (solvent B). A 90–minute gradient was used: 0–10 min, 2% B; 10–50 min, 2–35% B; 50–60 min, 35–90% B; 60–65 min, 90% B, 65–70 min, 90–2% B, 70–90 min, 2% B. The eluted peptides were analyzed on either LTQ Orbitrap XL or LTQ Orbitrap Velos mass spectrometers (Thermo Scientific), operated using a data-dependent method with dynamic exclusion enabled. Full scan (m/z 300–2000) spectra were acquired with the Orbitrap as the mass analyzer (resolution 60,000), and the five most abundant (LTQ Orbitrap XL) or twelve most abundant ions (LTQ Orbitrap Velos) in each MS scan were selected for fragmentation via collision-induced dissociation (CID) in the LTQ. For analyses performed on the LTQ Orbitrap XL, the data-dependent method included neutral loss triggered MS3 scan events, where MS3 scans were performed when neutral losses of 97.98, 48.99, or 32.66 (neutral losses specific for phosphorylation) were detected in the preceding MS2 spectra. All tandem mass spectra were converted into DTA files using Scansifter, and searched against a human subset of the UniProtKB protein database (uniprot.org), also containing reversed (decoy) protein sequences. Database searches were performed using a custom version of SEQUEST[3] on the Vanderbilt ACCRE Linux cluster, and results were assembled in Scaffold 3 (Proteome Software) with minimum filtering criteria of 95% peptide probability. All searches were configured to use variable modifications of carbamidomethylation on cysteine, oxidation of methionine, and phosphorylation of serine, threonine, and tyrosine. Sites of modification were validated by manual interpretation of the raw tandem mass spectra using QualBrowser software (Xcalibur 2.1.0, Thermo Scientific). To determine the relative abundance of phosphorylated peptides in digests of *in vitro* phosphorylated DGLα, accurate mass measurements acquired in the Orbitrap were used to generate extracted ion chromatograms (XICs). A window of 10 ppm around the theoretical monoisotopic m/z values of the observed precursor ions was utilized

for making XICs of the unmodified and phosphorylated peptide pairs. Using QualBrowser, the integrated area under each XIC peak was determined, and the percent relative abundance of each phosphorylated peptide was calculated as a percentage of the total area under the curve (AUC) obtained for both the phosphorylated and unmodified forms for each DGLα peptide. AUCs were calculated for the following phosphorylated peptides: DGLα residues 405–416, 741–751, 774–795, 805–815, 838–848, 859–874, 1021–1033, and 1021–1042.

For identification of protein in mouse striatal DGLα immune complexes, samples were resolved by SDS-PAGE and entire gel lanes were excised for in-gel trypsin digestion. All immune complex data were acquired on the LTQ Orbitrap XL mass spectrometer (Thermo Scientific). Data-dependent methods were used where the five most abundant ions were selected for fragmentation, and dynamic exclusion was applied. SEQUEST was similarly used for database searching against a Mus musculus subset of the UniProtKB protein database, concatenated with reversed (decoy) sequences. Resulting peptide identifications were assembled using IDPicker 2.6[4] with a target false discovery rate of 5% and a minimum requirement of two distinct peptides per protein.

Phosphorylation of two DGLα-V5 peptides, GSPSLHAVLER (residues 805–815), and RAPLATMESLSDTESLYSFDSR (residues 774–795) was analyzed using a targeted LC-MS/MS multiple-reaction monitoring (MRM) method, which was optimized using peptides derived from *in vitro* phosphorylated GST-DGLα (761–870) (see Fig. 2c/d). For these studies, DGLα-V5 was purified in the presence of protein phosphatase inhibitors from HEK293T cell lysates following co-expression with or without constitutively active CaMKIIα. DGLα-V5 was resolved via SDS-PAGE and in-gel digested with trypsin (see above) and then extracted peptides were resolved on a C18 column using a Waters NanoAcquity LC (flow rate: 450 nl/min). Peptides were eluted using a 60-min gradient (0–1 min, 1% B; 1–40 min, 1–40% B; 40–45 min, 40–90% B; 45–46 min, 90% B; 46–48 min, 90–1% B; 48–60 min, 1% B) and then analyzed on a TSQ Vantage triple quadrupole mass spectrometer, equipped with a nanoelectrospray ionization source (Thermo Scientific). Instrument method parameters included Q2 collision cell gas of 1.5 mTorr, 0.02 m/z scan width, scan time of 50 ms, and Q1 and Q3 resolution of 0.7 at FWHM. The targeted DGLα peptides and their corresponding precursor and product m/z values empirically developed for MRM analysis using *in vitro* phosphorylated DGLα is listed in Supplementary Table 2. This optimized method with a refined subset of selected MRM transitions for each peptide was then used to analyze DGLα that had been phosphorylated in intact cells (See Supplementary Figure 3). The MRM data were imported into Skyline software[5] for analysis, where co-eluting transition peaks were grouped by peptide precursor.

### *In Vitro* Phosphorylation Assay

DGLα-V5- or DGLβ-V5 bound to protein-G beads (see above) were incubated (20 min; 30°C) in the presence or absence of purified CaMKIIα (10 nM) in assay buffer (50 mM HEPES, pH 7.5, 10 mM $MgCl_2$, 2 mM $CaCl_2$, 2 μM calmodulin, 1 μM dithiothreitol, 400 μM [$\gamma$-$^{32}$P]ATP (700–1000 cpm/pmol)). Reactions were stopped and proteins eluted by heating (10 min; 70°C) in LDS sample buffer (Invitrogen). Proteins were resolved by SDS-PAGE and transferred to nitrocellulose membranes, which were then exposed overnight to

X-ray film. To verify expression and the specificity of immunoprecipitation, membranes were then western blotted with a mouse anti-V5 antibody. Essentially the same procedure was carried out in reactions involving GST-fusion proteins, except that 15 μl aliquots of the reactions were stopped on P82 Whatman paper. The papers were then washed and phosphorylation stoichiometries were determined by quantifying $^{32}P$ incorporation using a scintillation counter. To visualize phosphorylated products by autoradiography, some GST-fusion protein reactions were quenched with sample buffer and resolved by SDS-PAGE (see above).

### DGL Activity Assay

Mouse striata or transfected HEK293T cell pellets were dounce homogenized in lysis buffer containing 20 mM HEPES (pH 7.5), 2 mM DTT, 250 mM sucrose, 10 μg/ml leupeptin, 10 μg/ml pepstatin, 1 mM PMSF and 1 μM microcystin. Following homogenization, membranes were pelleted by centrifugation at 10,000×g for 25 min at 4°C. The membrane pellet was resuspended in a dounce homogenizer in membrane resuspension buffer containing 20 mM HEPES (pH 7.5), 2 mM DTT, 10 μg/ml leupeptin, 10 μg/ml pepstatin, 1 mM PMSF and 1 μM microcystin.

Aliquots of membrane protein (5 μg), containing equal levels of DGLα protein by immunoblot, were incubated (final volume: 50 μl. 37°C or room temperature, as indicated) with 1-steroyl-2-arachidonoylglycerol (SAG; Cayman Chemical), which was added directly from a 100% methanol stock (final methanol concentration: 5%). Reactions were stopped by adding 200 μl of 100% methanol containing 125 pmol 2-AG-$d_8$ and 50 pmol arachidonic acid-$d_8$. Insoluble material was removed by centrifugation (2000×g, 10 min, 4°C), and 20 μl of supernatant was analyzed by LC/MS.

### Analysis of eCBs and arachidonic acid in dorsolateral striatum

After rapid decapitation without anesthesia, 1.0 mm blocks of tissue containing pre-commisural striatum were rapidly frozen on dry ice. Punches (1.0 mm) of dorsolateral striatum were stored at −80°C. Tissue punches were homogenized by sonication in 100% acetonitrile spiked with 100 pmol 2-AG-$d_8$, 1 pmol anandamide-$d_8$ and 500 pmol arachidonic acid-$d_8$. After centrifugation (2000×g, 10 min, 4°C) to remove insoluble material, samples were dried under $N_2$ gas and stored at −80°C. The samples were resuspended in 9:1 methanol:$H_2O$ and subjected to LC/MS analysis.

### LC/MS detection of lipids

LC/MS detection of endocannabinoids and arachidonic acid was performed as previously described[6]. Briefly, sample (20 μl) was injected into a C-18 column (50 × 2 mm, 3 μm; Phenomenex) under the following gradient: 20% A and 80% B from 0 to 0.5 min, increased to 0% A and 100% B from 0.5 to 3.5 min and held for 1 min, and 20% A and 80% B from 4.5 to 6.5. Component A is water and B is methanol, and each component contained 80 μM silver acetate and 0.5% acetic acid (v/v). Analytes were detected via selective reaction monitoring (as [M+Ag]+ complexes except AA, which is ionized as [(M-H)+2Ag]+) in the positive ion mode using the following reactions (the mass in parentheses represents the mass of the deuterated internal standard): AA (m/z 519(527) → 409(417)); 2-AG (m/z 485(493)

→ 411(419)); and AEA (m/z 454(462) → 432(440)). Quantification was achieved via stable isotope dilution for AA, 2-AG, and AEA. Levels of analytes are given in pmols/fmol of analyte per mg wet tissue weight for striatal measurements or pmol per μg protein for DGL activity assays.

## Brain Slice Preparation and electrophysiology

Mice were anesthetized using isoflurane prior to decapitation and slicing. Brains were hemisected, and slices (300 μm) were made using a Leica VT1000S vibratome (Leica Microsystems) in oxygenated (95% v/v $O_2$, 5% v/v $CO_2$) ACSF maintained at 1–4 °C (in mM: 208 sucrose, 2.5 KCl, 1 $CaCl_2$, 4 $MgCl_2$, 4 MgSO4, 1.6 $NaH_2PO_4$, 26 $NaHCO_3$, 10 glucose, 1 ascorbate, 3 Na-pyruvate).

Electrophysiological recordings were performed at 30°C in oxygenated ACSF ((in mM) 113 NaCl, 2.5 KCl, 2.5 CaCl2, 1.2 MgSO4, 1 $NaH_2PO_4$, 26 $NaHCO_3$, 20 glucose, 1 ascorbate, 3 Na-pyruvate) containing picrotoxin (50 μM) continuously perfused at 2 ml/min. Patch electrodes (2–4 MΩ) were filled with pipette solution consisting of (in mM): 120 K-gluconate, 4 NaCl, 10 HEPES, 20 KCl, 4 Mg-ATP, and 0.3 Na-GTP, 10 Na-phosphocreatine with pH adjusted to 7.2 with KOH. Whole cell voltage-clamp recordings in visually identified D2-eGPF positive [D2(+)] and D2-eGFP negative [D2(−)] MSNs located were performed in the dorsolateral striatum. D2(−) MSNs were defined as cells having no detectable fluorescence. Baseline evoked EPSCs (eEPSCs) were elicited by stimulation through an ACSF-filled glass pipette placed ~100 μm dorsolateral of the patched cell. Stimulation pulses were delivered every 5 sec prior to and immediately following application of a postsynaptic depolarization (+30 mV; 2–10 sec, as indicated) in an attempt to induce DSE. This paradigm was repeated three times on each cell, and normalized eEPSC amplitudes were averaged for each cell. Responses were normalized to an average of the baseline responses. Average normalized response amplitudes during the baseline were compared to the first time point following depolarization and statistical significance between groups was determined by an unpaired Student's t-test unless otherwise indicated. Series and input resistance was monitored throughout the experiment and recordings were discarded if series resistance changed by >20%.

## Homecage Behavioral Monitoring

All mice were housed separately for 48 hours prior to and throughout homecage monitoring. WT littermates or T286A-KI mice were given an IP vehicle (1:1:18 ethanol:emulphor:saline) injection 30 minutes before the beginning of the dark cycle and were monitored continuously for the next 24 hours. The following day, the same mice were given a 12 mg/kg dose of JZL-184 (Cayman Chemical, Ann Arbor, MI) 30 minutes prior to the dark cycle. Inhibition of MAGL by JZL-184 was reported to elevate brain 2-AG levels for more than 8 hours[7]. The automated Homecage Analysis monitoring system (CleverSys Inc.) was set to monitor distance traveled as well as several other relevant behaviors. The time spent eating and drinking were defined as time spent at the food bin or water bottle. Significance was determined by 2-way ANOVA, which was followed by Bonferroni's posthoc test to compare groups if the 2-way ANOVA revealed a significant interaction.

### Statistics

The statistical tests and parameters used are indicated in figure legends. Results were considered significant if they reached $p < 0.05$. Sample sizes for each experiment are based on previously published studies from our laboratories[2, 6, 8]. No blinding was done in any experiments. All data are presented as mean±s.e.m.

## Supplementary Material

Refer to Web version on PubMed Central for supplementary material.

## Acknowledgments

Supported by the NIH (T32-NS007491, T32-MH065215 to BCS; K01-NS073700 to AJB; K05-DA021696, R01-DA011322 to KM; RO1-AA019455 to DGW; K08-MH090412 to SP; R01-MH063232, R01-NS078291 to RJC), the Michael J. Fox Foundation (RJC), and the Luton Society (SP). Behavioral studies were performed in the Murine Neurobehavior Core and mass spectrometry and proteomics studies were performed at the Mass Spectrometry Research Center, both at Vanderbilt University Medical Center.

We thank Dr. Benjamin Cravatt for generously providing DGLα-V5 and DGLβ-V5 plasmids.

## References

1. Graybiel AM, Aosaki T, Flaherty AW, Kimura M. The basal ganglia and adaptive motor control. Science. 1994; 265:1826–1831. [PubMed: 8091209]
2. Packard MG, Knowlton BJ. Learning and memory functions of the Basal Ganglia. Annu Rev Neurosci. 2002; 25:563–593. [PubMed: 12052921]
3. Kravitz AV, Tye LD, Kreitzer AC. Distinct roles for direct and indirect pathway striatal neurons in reinforcement. Nat Neurosci. 2012
4. Gerdeman GL, Ronesi J, Lovinger DM. Postsynaptic endocannabinoid release is critical to long-term depression in the striatum. Nat Neurosci. 2002; 5:446–451. [PubMed: 11976704]
5. Kreitzer AC, Malenka RC. Dopamine modulation of state-dependent endocannabinoid release and long-term depression in the striatum. J Neurosci. 2005; 25:10537–10545. [PubMed: 16280591]
6. Shen YS, Gao H, Yao H. Spike timing-dependent synaptic plasticity in visual cortex: a modeling study. J Comput Neurosci. 2005; 18:25–39. [PubMed: 15789167]
7. Tanimura A, et al. The endocannabinoid 2-arachidonoylglycerol produced by diacylglycerol lipase alpha mediates retrograde suppression of synaptic transmission. Neuron. 2010; 65:320–327. [PubMed: 20159446]
8. Wilson RI, Kunos G, Nicoll RA. Presynaptic specificity of endocannabinoid signaling in the hippocampus. Neuron. 2001; 31:453–462. [PubMed: 11516401]
9. Di Filippo M, et al. The endocannabinoid system in Parkinson's disease. Curr Pharm Des. 2008; 14:2337–2347. [PubMed: 18781984]
10. Muller-Vahl KR, Schneider U, Kolbe H, Emrich HM. Treatment of Tourette's syndrome with delta-9-tetrahydrocannabinol. Am J Psychiatry. 1999; 156:495. [PubMed: 10080574]
11. Blazquez C, et al. Loss of striatal type 1 cannabinoid receptors is a key pathogenic factor in Huntington's disease. Brain. 2011; 134:119–136. [PubMed: 20929960]
12. Devane WA, Axelrod J. Enzymatic synthesis of anandamide, an endogenous ligand for the cannabinoid receptor, by brain membranes. Proc Natl Acad Sci U S A. 1994; 91:6698–6701. [PubMed: 8022836]
13. Sugiura T, et al. 2-Arachidonoylglycerol: a possible endogenous cannabinoid receptor ligand in brain. Biochem Biophys Res Commun. 1995; 215:89–97. [PubMed: 7575630]
14. Ade KK, Lovinger DM. Anandamide regulates postnatal development of long-term synaptic plasticity in the rat dorsolateral striatum. J Neurosci. 2007; 27:2403–2409. [PubMed: 17329438]

15. Oudin MJ, Hobbs C, Doherty P. DAGL-dependent endocannabinoid signalling: roles in axonal pathfinding, synaptic plasticity and adult neurogenesis. Eur J Neurosci. 2011; 34:1634–1646. [PubMed: 22103420]
16. Yoshino H, et al. Postsynaptic diacylglycerol lipase alpha mediates retrograde endocannabinoid suppression of inhibition in mouse prefrontal cortex. J Physiol. 2011
17. Gao Y, et al. Loss of retrograde endocannabinoid signaling and reduced adult neurogenesis in diacylglycerol lipase knock-out mice. J Neurosci. 2010; 30:2017–2024. [PubMed: 20147530]
18. Bisogno T, et al. Cloning of the first sn1-DAG lipases points to the spatial and temporal regulation of endocannabinoid signaling in the brain. J Cell Biol. 2003; 163:463–468. [PubMed: 14610053]
19. Jung KM, et al. A key role for diacylglycerol lipase-alpha in metabotropic glutamate receptor-dependent endocannabinoid mobilization. Mol Pharmacol. 2007; 72:612–621. [PubMed: 17584991]
20. Uchigashima M, et al. Subcellular arrangement of molecules for 2-arachidonoylglycerol-mediated retrograde signaling and its physiological contribution to synaptic modulation in the striatum. J Neurosci. 2007; 27:3663–3676. [PubMed: 17409230]
21. Lerner TN, Kreitzer AC. RGS4 is required for dopaminergic control of striatal LTD and susceptibility to Parkinsonian motor deficits. Neuron. 2012; 73:347–359. [PubMed: 22284188]
22. Lerner TN, Horne EA, Stella N, Kreitzer AC. Endocannabinoid signaling mediates psychomotor activation by adenosine A2A antagonists. J Neurosci. 2012; 30:2160–2164. [PubMed: 20147543]
23. Wilson RI, Nicoll RA. Endogenous cannabinoids mediate retrograde signalling at hippocampal synapses. Nature. 2001; 410:588–592. [PubMed: 11279497]
24. Kreitzer AC, Regehr WG. Retrograde signaling by endocannabinoids. Curr Opin Neurobiol. 2002; 12:324–330. [PubMed: 12049940]
25. Kreitzer AC, Regehr WG. Retrograde inhibition of presynaptic calcium influx by endogenous cannabinoids at excitatory synapses onto Purkinje cells. Neuron. 2001; 29:717–727. [PubMed: 11301030]
26. Ohno-Shosaku T, Maejima T, Kano M. Endogenous cannabinoids mediate retrograde signals from depolarized postsynaptic neurons to presynaptic terminals. Neuron. 2001; 29:729–738. [PubMed: 11301031]
27. Hashimotodani Y, et al. Phospholipase Cbeta serves as a coincidence detector through its Ca2+ dependency for triggering retrograde endocannabinoid signal. Neuron. 2005; 45:257–268. [PubMed: 15664177]
28. Maejima T, et al. Synaptically driven endocannabinoid release requires Ca2+-assisted metabotropic glutamate receptor subtype 1 to phospholipase Cbeta4 signaling cascade in the cerebellum. J Neurosci. 2005; 25:6826–6835. [PubMed: 16033892]
29. Maejima T, Ohno-Shosaku T, Kano M. Endogenous cannabinoid as a retrograde messenger from depolarized postsynaptic neurons to presynaptic terminals. Neurosci Res. 2001; 40:205–210. [PubMed: 11448511]
30. Robison AJ, Bartlett RK, Bass MA, Colbran RJ. Differential modulation of Ca2+/calmodulin-dependent protein kinase II activity by regulated interactions with N-methyl-D-aspartate receptor NR2B subunits and alpha-actinin. J Biol Chem. 2005; 280:39316–39323. [PubMed: 16172120]
31. Robison AJ, et al. Multivalent interactions of calcium/calmodulin-dependent protein kinase II with the postsynaptic density proteins NR2B, densin-180, and alpha-actinin-2. J Biol Chem. 2005; 280:35329–35336. [PubMed: 16120608]
32. Miller SG, Kennedy MB. Regulation of brain type II Ca2+/calmodulin-dependent protein kinase by autophosphorylation: a Ca2+-triggered molecular switch. Cell. 1986; 44:861–870. [PubMed: 3006921]
33. Nikandrova YA, Jiao Y, Baucum AJ, Tavalin SJ, Colbran RJ. Ca2+/calmodulin-dependent protein kinase II binds to and phosphorylates a specific SAP97 splice variant to disrupt association with AKAP79/150 and modulate alpha-amino-3-hydroxy-5-methyl-4-isoxazolepropionic acid-type glutamate receptor (AMPAR) activity. J Biol Chem. 2010; 285:923–934. [PubMed: 19858198]
34. Grueter CE, et al. L-type Ca2+ channel facilitation mediated by phosphorylation of the beta subunit by CaMKII. Mol Cell. 2006; 23:641–650. [PubMed: 16949361]

35. Giese KP, Fedorov NB, Filipkowski RK, Silva AJ. Autophosphorylation at Thr286 of the alpha calcium-calmodulin kinase II in LTP and learning. Science. 1998; 279:870–873. [PubMed: 9452388]
36. Miller SG, Patton BL, Kennedy MB. Sequences of autophosphorylation sites in neuronal type II CaM kinase that control Ca2(+)-independent activity. Neuron. 1988; 1:593–604. [PubMed: 2856100]
37. Dinh TP, et al. Brain monoglyceride lipase participating in endocannabinoid inactivation. Proc Natl Acad Sci U S A. 2002; 99:10819–10824. [PubMed: 12136125]
38. Ohno-Shosaku T, Hashimotodani Y, Maejima T, Kano M. Calcium signaling and synaptic modulation: regulation of endocannabinoid-mediated synaptic modulation by calcium. Cell Calcium. 2005; 38:369–374. [PubMed: 16085309]
39. Kreitzer AC, Malenka RC. Endocannabinoid-mediated rescue of striatal LTD and motor deficits in Parkinson's disease models. Nature. 2007; 445:643–647. [PubMed: 17287809]
40. Shen W, Flajolet M, Greengard P, Surmeier DJ. Dichotomous dopaminergic control of striatal synaptic plasticity. Science. 2008; 321:848–851. [PubMed: 18687967]
41. Gong S, et al. A gene expression atlas of the central nervous system based on bacterial artificial chromosomes. Nature. 2003; 425:917–925. [PubMed: 14586460]
42. Maejima T, Hashimoto K, Yoshida T, Aiba A, Kano M. Presynaptic inhibition caused by retrograde signal from metabotropic glutamate to cannabinoid receptors. Neuron. 2001; 31:463–475. [PubMed: 11516402]
43. Aravanis AM, et al. An optical neural interface: in vivo control of rodent motor cortex with integrated fiberoptic and optogenetic technology. J Neural Eng. 2007; 4:S143–156. [PubMed: 17873414]
44. Wiley JL, Martin BR. Cannabinoid pharmacological properties common to other centrally acting drugs. Eur J Pharmacol. 2003; 471:185–193. [PubMed: 12826237]
45. Long JZ, et al. Selective blockade of 2-arachidonoylglycerol hydrolysis produces cannabinoid behavioral effects. Nat Chem Biol. 2009; 5:37–44. [PubMed: 19029917]
46. Zhang L, Wang M, Bisogno T, Di Marzo V, Alger BE. Endocannabinoids generated by Ca2+ or by metabotropic glutamate receptors appear to arise from different pools of diacylglycerol lipase. PLoS ONE. 2011; 6:e16305. [PubMed: 21305054]
47. Jenkins MA, et al. Ca2+-dependent facilitation of Cav1.3 Ca2+ channels by densin and Ca2+/calmodulin-dependent protein kinase II. J Neurosci. 2010; 30:5125–5135. [PubMed: 20392935]
48. Gustin RM, et al. Loss of Thr286 phosphorylation disrupts synaptic CaMKIIalpha targeting, NMDAR activity and behavior in pre-adolescent mice. Mol Cell Neurosci. 2011; 47:286–292. [PubMed: 21627991]
49. Picconi B, et al. Abnormal Ca2+-calmodulin-dependent protein kinase II function mediates synaptic and motor deficits in experimental parkinsonism. J Neurosci. 2004; 24:5283–5291. [PubMed: 15190099]
50. Brown AM, Deutch AY, Colbran RJ. Dopamine depletion alters phosphorylation of striatal proteins in a model of Parkinsonism. Eur J Neurosci. 2005; 22:247–256. [PubMed: 16029214]

## References

1. Giese KP, Fedorov NB, Filipkowski RK, Silva AJ. Autophosphorylation at Thr286 of the alpha calcium-calmodulin kinase II in LTP and learning. Science. 1998; 279:870–873. [PubMed: 9452388]
2. Robison AJ, Bartlett RK, Bass MA, Colbran RJ. Differential modulation of Ca2+/calmodulin-dependent protein kinase II activity by regulated interactions with N-methyl-D-aspartate receptor NR2B subunits and alpha-actinin. J Biol Chem. 2005; 280:39316–39323. [PubMed: 16172120]
3. Eng JK, McCormack AL, Yates I, John R. An approach to correlate tandem mass spectral data of peptides with amino acid sequences in a protein database. J. Am. Soc. Mass Spectrom. 1994; 5:976–989. [PubMed: 24226387]
4. Ma ZQ, et al. IDPicker 2.0: Improved protein assembly with high discrimination peptide identification filtering. J Proteome Res. 2009; 8:3872–3881. [PubMed: 19522537]

5. MacLean B, et al. Skyline: an open source document editor for creating and analyzing targeted proteomics experiments. Bioinformatics. 2010; 26:966–968. [PubMed: 20147306]
6. Patel S, Kingsley PJ, Mackie K, Marnett LJ, Winder DG. Repeated homotypic stress elevates 2-arachidonoylglycerol levels and enhances short-term endocannabinoid signaling at inhibitory synapses in basolateral amygdala. Neuropsychopharmacology. 2009; 34:2699–2709. [PubMed: 19675536]
7. Long JZ, et al. Selective blockade of 2-arachidonoylglycerol hydrolysis produces cannabinoid behavioral effects. Nat Chem Biol. 2009; 5:37–44. [PubMed: 19029917]
8. Sumislawski JJ, Ramikie TS, Patel S. Reversible gating of endocannabinoid plasticity in the amygdala by chronic stress: a potential role for monoacylglycerol lipase inhibition in the prevention of stress-induced behavioral adaptation. Neuropsychopharmacology. 2011; 36:2750–2761. [PubMed: 21849983]

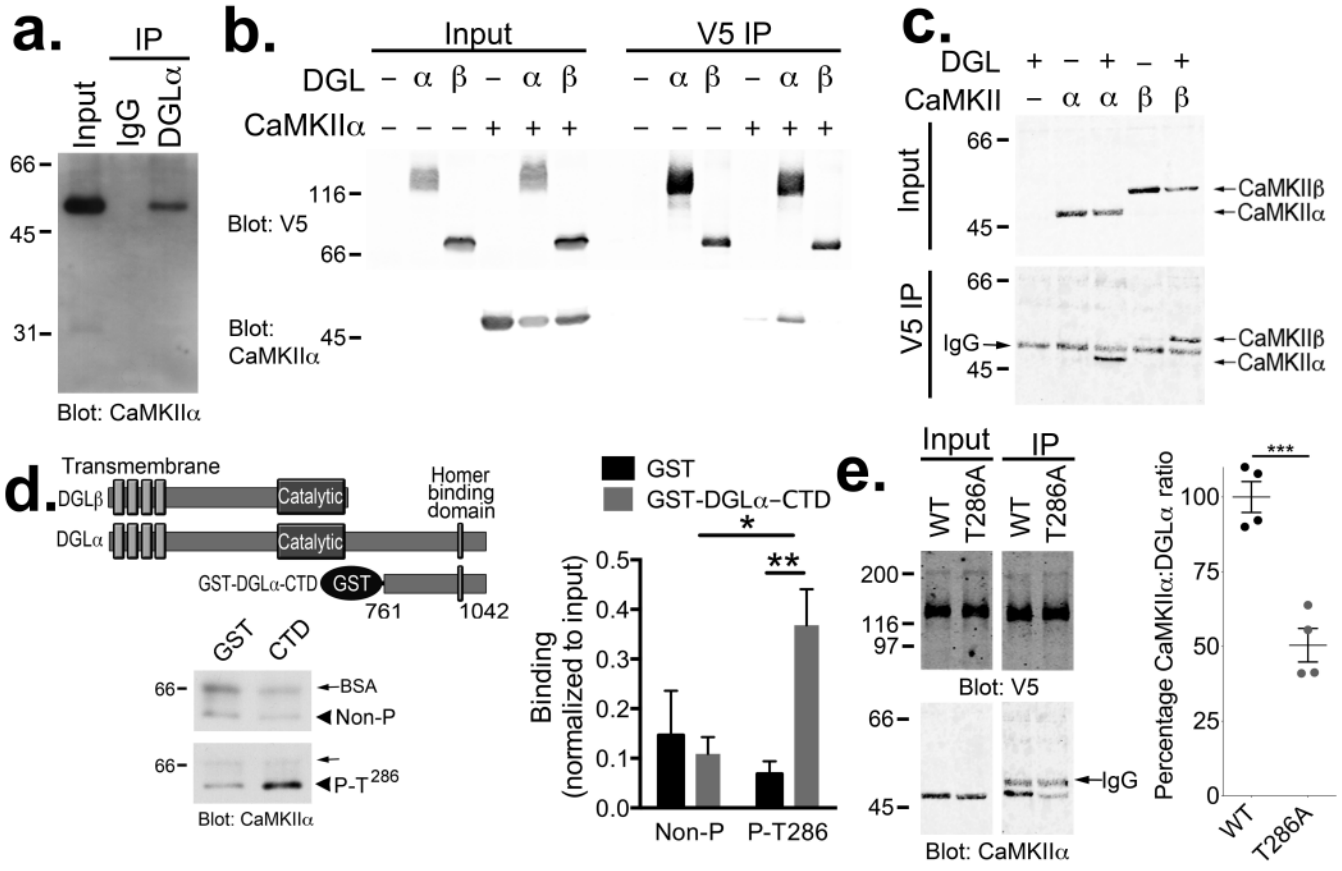


**Figure 1. DGLα interacts with CaMKII**

**(a)** Western blot confirms that CaMKIIα specifically associates with DGLα immune complexes, but not control IgG complexes, isolated from mouse striatal extracts. **(b)** CaMKIIα was detected in DGLα-V5 but not DGLβ-V5 immune complexes isolated from co-transfected HEK293T cells. Control cells were not transfected or expressed either CaMKIIα or DGLα/β-V5 alone. **(c)** Both CaMKII-α and -β associated with DGLα-V5 immune complexes isolated from co-transfected HEK293T cells. The band between CaMKII-α and -β in all of the IP samples is the IgG heavy chain used for the immunoprecipitation, as indicated. Panels a–c are representative of at least two experiments. **(d)** Alignment of DGLα and DGLβ highlights a unique C-terminal domain in DGLα. A GST fusion protein containing the C-terminal domain (CTD; residues 761–1042) of DGLα directly interacts with purified $Thr^{286}$-autophosphorylated, but not non-phosphorylated, CaMKIIα *in vitro*. The amount of CaMKII detected in each sample was normalized to the amount detected in an aliquot of the input for each incubation (Non-P (n=5 independent experiments): 0.15±0.09 and 0.11±0.03 for GST and GST-DGLα-CTD, respectively. P-T286 (n=6 independent experiments): 0.07±0.03 and 0.37±0.07 for GST and GST-DGLα-CTD, respectively. 2-way ANOVA: Interaction, $F(1,18)=7.739$, $P=0.0123$. Autophosphorylation, $F_{1,18}=4.661$, $P=0.0446$. Protein, $F_{1,18}=2.226$, $P=0.1530$. Tukey's post-test: *, $p<0.05$; **, $p<0.01$). **(e)** The interaction of CaMKIIα with DGLα-V5 in cotransfected HEK293T cells was significantly reduced by mutating $Thr^{286}$ to Ala in

CaMKIIα (WT=100±5%, n=4 independent experiments; T286A=50±6%, n=4 independent experiments; *** $t_6$=6.494, $p$<0.001 unpaired two-tailed t-test).

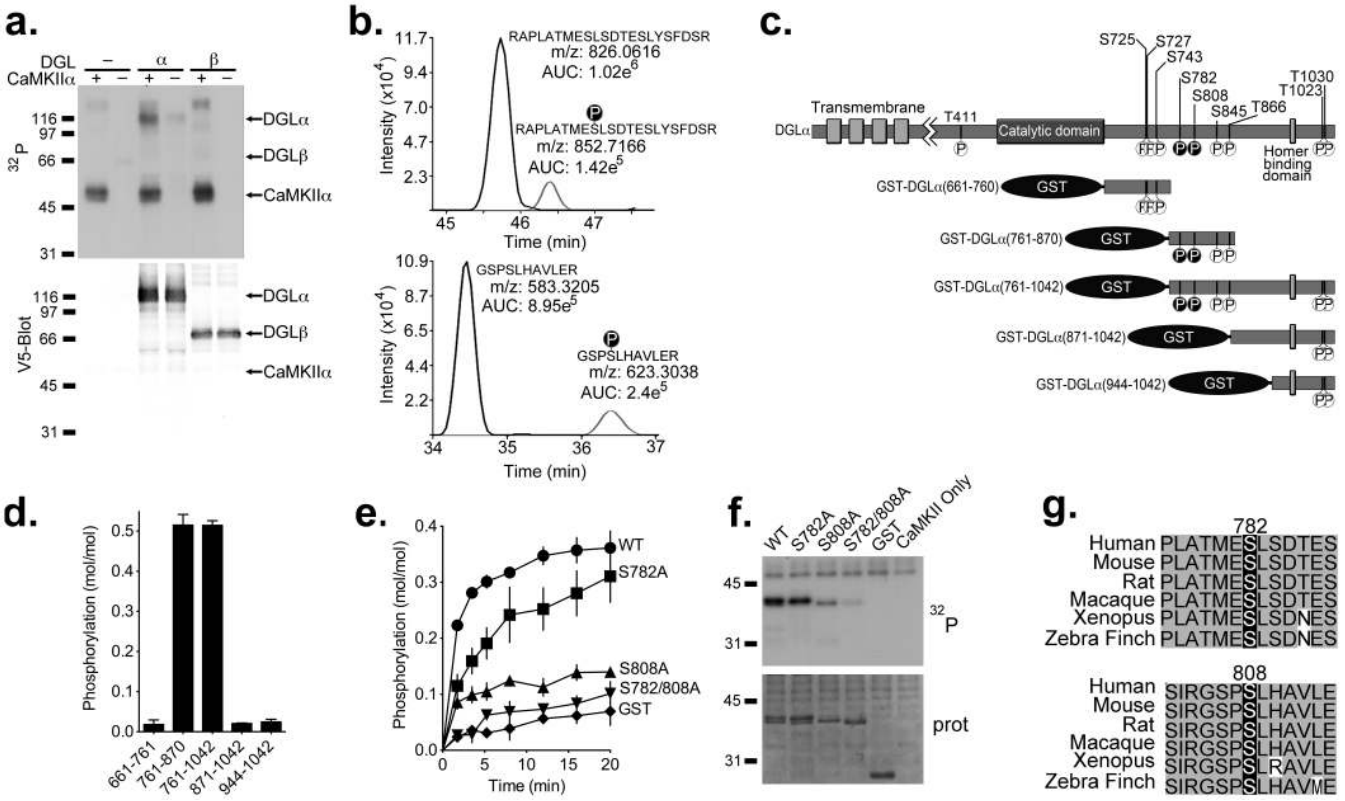


**Figure 2. CaMKIIα selectively phosphorylates DGLα at Ser$^{782}$ and Ser$^{808}$**

**(a)** Purified DGLα/β-V5 was incubated with [γ-$^{32}$P]ATP and recombinant CaMKIIα and analyzed by SDS-PAGE. The ~116 kDa $^{32}$P-labeled band on the autoradiograph ($^{32}$P) overlaps with the DGLα-V5 band shown on the corresponding V5 western blot (Blot: V5), and was not detected in the absence of CaMKIIα or DGLα-V5. DGLβ-V5 was not significantly $^{32}$P-phosphorylated. **(b)** Extracted ion chromatograms are shown for phosphorylated and non-phosphorylated DGLα peptides containing Ser$^{782}$ and Ser$^{808}$. The monoisotopic m/z values for the observed $[M+3H]^{3+}$ and $[M+2H]^{2+}$ precursor ions for DGLα peptides 774–795 (top) and 805–815 (bottom), respectively, are provided adjacent to their corresponding chromatographic peak. Observed values are within 2 ppm of theoretical values calculated for these precursor ions. **(c)** Phosphorylation sites identified by mass spectrometric analysis of full length WT DGLα purified from HEK293 cells are indicated (see Table 1). The two CaMKII-specific sites, Ser$^{782}$ and Ser$^{808}$ are indicated with black circles. GST-fusion proteins used in panel d are also shown. **(d)** GST-fusion proteins containing C-terminal tail fragments of DGLα were incubated with recombinant CaMKIIα and [γ-$^{32}$P]ATP. CaMKII selectively phosphorylated fragments containing amino acids 761–870. **(e)** Time course for phosphorylation of GST-DGLα (761–870) (WT, S782A, S808A or S782A/S808A) or GST alone by CaMKIIα. **(f)** Representative autoradiograph ($^{32}$P) and protein stain (prot) of SDS-PAGE analysis of reactions from panel (e) at 10 min. (**g**) Ser$^{782}$ and Ser$^{808}$ are conserved in a range of vertebrates.

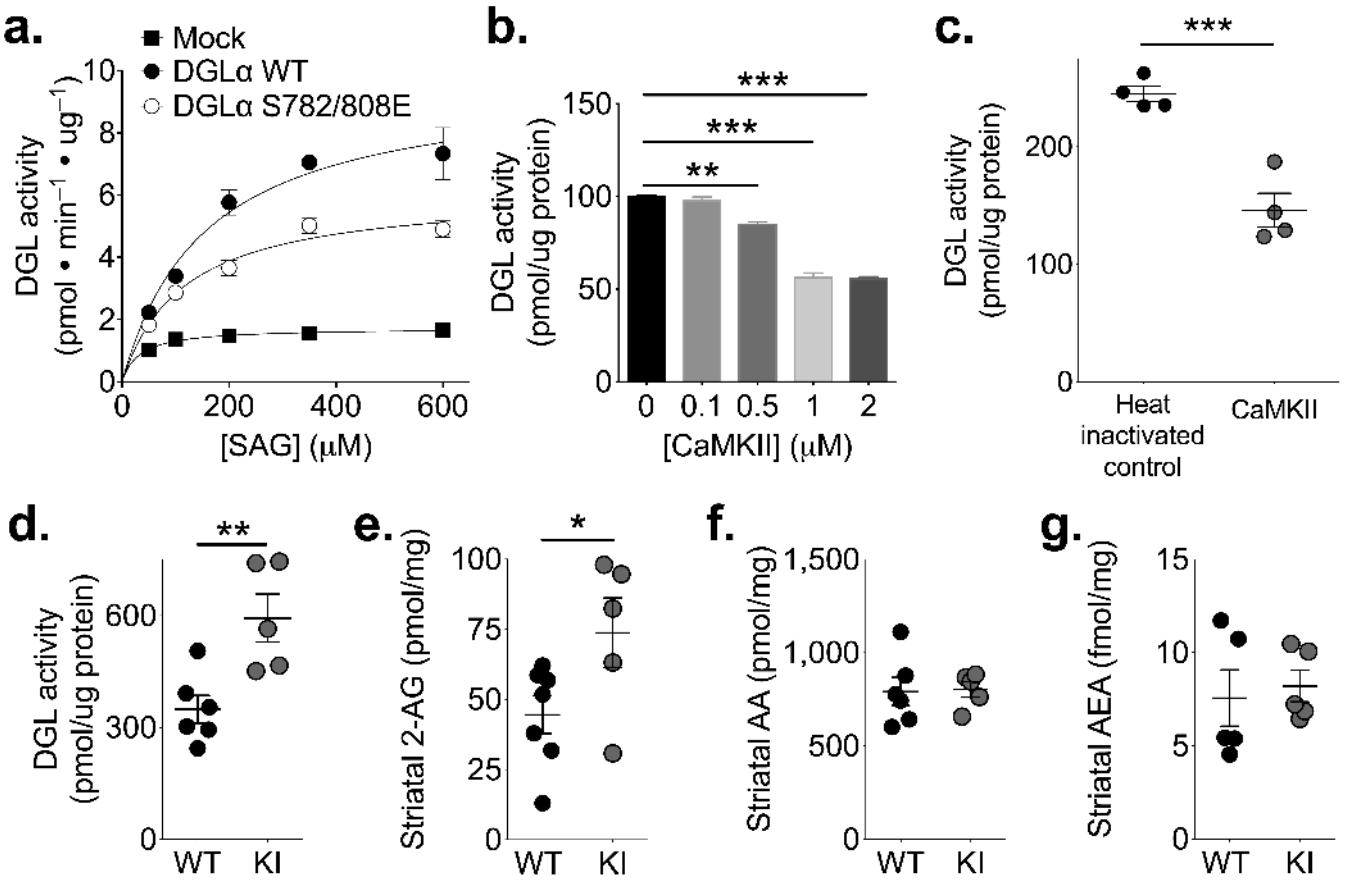


**Figure 3. CaMKII inhibits DGL activity**

**(a)** Phosphomimetic mutation of $Ser^{782}$ and $Ser^{808}$ to glutamate decreased the $V_{max}$ in membranes from DGLα-V5 transfected HEK293T cells without a significant effect on $K_m$ (n=4 independent experiments; $V_{max}$ (pmol/min/μg): WT 9.8±1.1; S782/808E 6.1±0.4; unpaired two-tailed t-test: $t_6$=3.059, p=0.022; $K_m$ (μM): WT 158±24; S782/808A 114±8.7, p>0.05). Subtraction of the low activity in mock-transfected cell membranes (shown for comparison) from estimated $V_{max}$ values in transfected cell membranes indicates that the phosphomimetic mutations reduce DGLα activity by approximately 40%. **(b)** The addition of purified recombinant CaMKIIα to striatal membranes in the presence of $Ca^{2+}$, calmodulin, ATP and $Mg^{2+}$ resulted in concentration-dependent inhibition of DGL ([in pmol/μg protein] 0 nM 100.0±0.8; 100 nM 97.7±2.0; 500 nM 85.1±1.1; 1 μM 56.2±2.7; 2 μM 55.4±2.3; n=4 independent experiments; 1-way ANOVA $F_{4,10}$=161.8, p<0.0001; Bonferoni post-test: 0 vs 0.1: $t_{10}$=0.9609, p>0.05; 0 vs 0.05: $t_{10}$=6.16, **p<0.01; 0 vs 1: $t_{10}$=18.07, ***p<0.001; 0 vs 2: t10=18.38, ***p<0.001). **(c)** Prior heat treatment of CaMKIIα (1 μM) prevented the inhibition of DGL activity in striatal membranes ([in pmol/μg protein] heat inactivated CaMKIIα 244.9±6.5; active CaMKIIα 146.0±14.5; unpaired two tailed t-test: $t_6$=6.245, p=0.0008, n=4 independent experiments). **(d)** DGLα activity was significantly higher in striatal membranes from T286A-KI mice (KI) relative to WT littermates (WT 349±38 pmol/μg protein, n=6 mice; KI 594±64 pmol/μg protein, n=5 mice; unpaired two-tailed t-test: $t_9$=3.440, p=0.0074). **(e)** Total 2-AG levels in dorsolateral striatal punches were significantly higher in T286A-KI mice (KI) than in WT littermates ([in

pmol/mg tissue] WT 44.6±6.8, n=7 mice; KI 73.8±12.4, n=6 mice; unpaired two-tailed t-test: $t_{11}$=2.396, p=0.0355). **(f, g)** The levels of arachidonic acid **(f)** and anandamide (AEA) **(g)** were not significantly different between WT and T286A-KI mice (unpaired two-tailed t-test, p>0.05). *p<0.05, **p<0.01, ***p<0.001.

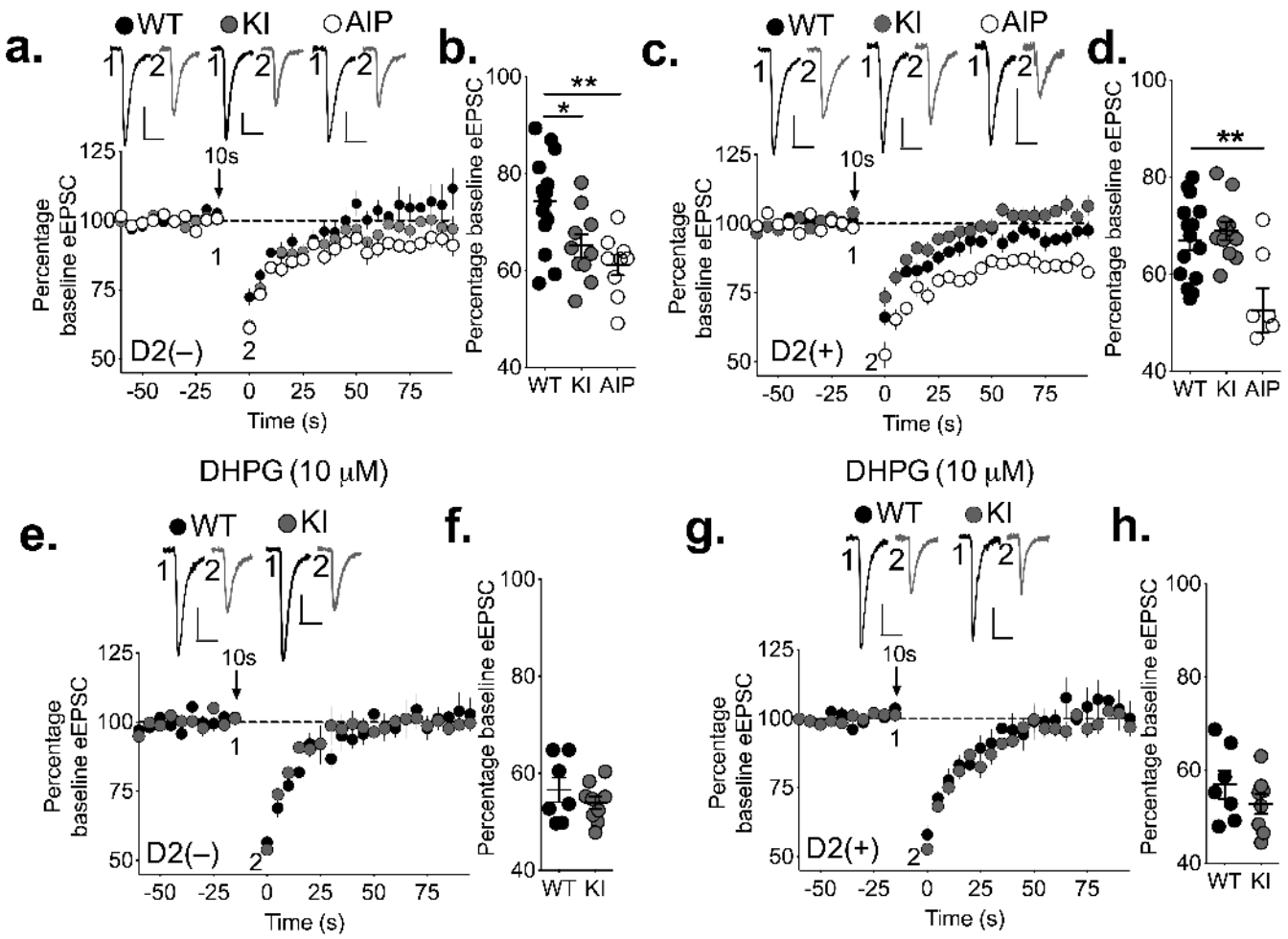


**Figure 4. Inhibiting CaMKII or preventing CaMKII autophosphorylation at Thr$^{286}$ enhances endocannabinoid-mediated retrograde transmission in striatal MSNs**

**(a,b)** DSE is significantly enhanced in D2(−) MSNs from T286A-KI (KI) mice (gray) relative to WT (black), and when the CaMKII inhibitory peptide AIP (10 μM; white) is included in the patch pipette (WT 74±2%, n=15 cells from 4 mice; KI 65±2%, n=10 cells from 4 mice; AIP 61±2%, n=9 cells from 3 mice; 1-way ANOVA: $F(2,31)=8.30$, $p=0.0013$; Bonferroni's post-test: WT vs. KI $t_{31}=2.764$, *$p<0.05$; WT vs. AIP $t_{31}=3.830$, **$p<0.01$). **(c,d)** In D2(+) MSNs, DSE was similar in WT and T286A-KI MSNs (gray), but loading AIP in WT cells significantly enhanced DSE (WT 67±2%, n=15 cells from 4 mice; KI 69±2%, n=11 cells from 5 mice; AIP 53±5%, n=7 cells from 3 mice. 1-way ANOVA: $F_{2,30}=8.769$, $p=0.001$. Bonferroni's post-test: WT vs. KI $t_{30}=0.5626$, $p>0.05$. WT vs. AIP $t_{30}=3.654$, **$p<0.01$). **(e, f)** Pretreatment of slices with DHPG (10 μM) enhanced DSE in D2(−) MSNs and prevented differences between WT and T286A-KI mice with 10 s depolarization (WT 57±3%, n=7 cells from 3 mice; KI 54±1, n=9 cells from 3 mice; unpaired two-tailed t-test, $p>0.05$). **(g, h)** Addition of DHPG also enhanced DSE in D2(+) MSNs but did not reveal differences between WT and T286A-KI mice with 10 s depolarization (WT 57±3%, n=7 cells from 4 mice; KI 53±2, n=8 cells from 4 mice; unpaired two-tailed t-test, $p>0.05$). Representative traces are shown for each condition. Calibration bars 20 ms × 150 pA.

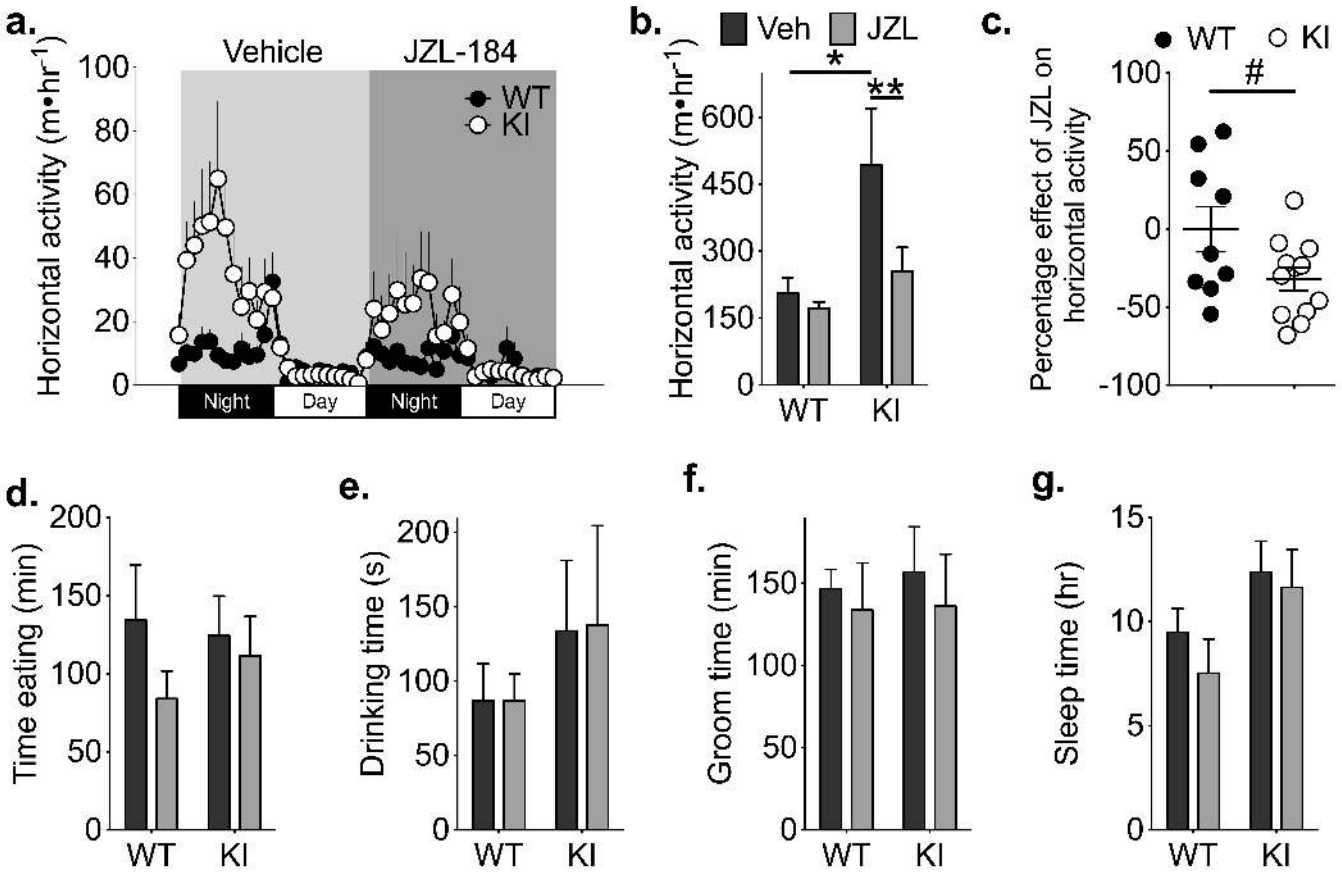


**Figure 5. Inhibition of 2-AG breakdown selectively suppresses motor activity in T286A-KI mice**

WT (n=9 mice) and T286A-KI (KI) (n=12 mice) mice were monitored for 24 h in their homecage after a vehicle injection, then treated with a submaximal dose of the MGL inhibitor JZL-184 (12 mg/kg ip; JZL) and monitored for an additional 24 hours. **(a)** The average horizontal activity in 1 h bins over time is plotted for the duration of the experiment, and the time of treatment with the vehicle and JZL-184 is indicated. **(b)** The average total horizontal activity in 24 h after injecting vehicle (Veh; black) or JZL-184 (JZL; gray). 2-way ANOVA; Interaction: $F_{1,17} = 5.40$, p=0.0328; Effect of Genotype: $F_{1,17} = 3.69$, p=0.0715; Effect of Drug: $F_{1,17} = 9.62$, p=0.0065. Sidak's post-test; * p<0.05, ** p<0.01. **(c)** Scatter plot showing horizontal activity of individual mice after treatment with JZL-184 as a percentage of activity during the vehicle-treatment phase. Unpaired two-tailed t-test; $t_{19}$=2.139, p=0.0456. **(d–g)** There were no significant effects of genotype or JZL-184 on **(d)** eating time, **(e)** drinking time, **(f)** grooming time or **(g)** sleeping time in the home cage (2-way ANOVA, p>0.05).

## Table 1

### Detection of DGLα phosphorylation sites

DGLα-V5 was immunoprecipitated from HEK293T cell lystates and incubated with Mg.ATP, calcium and calmodulin in the absence or presence of purified CaMKIIα. LC-MS/MS analysis detected phosphorylation at the sites listed, and the percentage phosphorylation at each site was estimated as the relative abundance of the phosphorylated peptide relative to the total area calculated for both non-phosphorylated and phosphorylated peptides. “ND” indicates that the peptide was not detected. “CD” indicates that the peptide and phosphorylation site were identified but the peptide was not present at a sufficient level to calculate relative abundance.

| | Percentage phosphorylated | |
|---|---|---|
| **Residue** | **– CaMKIIα** | **+ CaMKIIα** |
| Thr411 | 0.27 | 0.22 |
| Ser725 | CD | CD |
| Ser727 | CD | CD |
| Ser743 | 42.4 | 27.5 |
| **Ser782** | **ND** | **12.0** |
| **Ser808** | **ND** | **21.2** |
| Ser845 | 0.16 | 0.72 |
| Thr866 | 2.4 | 2.5 |
| Thr1023 | 5.7 | 4.4 |
| Ser1030 | 1.9 | 2.0 |